

UCSF

UC San Francisco Previously Published Works

Title

Uncapping and Deregulation of Telomeres Lead to Detrimental Cellular Consequences in Yeast

Permalink

<https://escholarship.org/uc/item/08r4w3h5>

Journal

Journal of Cell Biology, 145(2)

ISSN

0021-9525

Authors

Smith, Christopher D
Blackburn, Elizabeth H

Publication Date

1999-04-19

DOI

10.1083/jcb.145.2.203

Peer reviewed

Uncapping and Deregulation of Telomeres Lead to Detrimental Cellular Consequences in Yeast

Christopher D. Smith and Elizabeth H. Blackburn

Department of Microbiology & Immunology, University of California, San Francisco, San Francisco, CA 94143-0414

Abstract. Telomeres are the protein–nucleic acid structures at the ends of eukaryote chromosomes. Tandem repeats of telomeric DNA are templated by the RNA component (*TER1*) of the ribonucleoprotein telomerase. These repeats are bound by telomere binding proteins, which are thought to interact with other factors to create a higher-order cap complex that stabilizes the chromosome end. In the budding yeast *Kluyveromyces lactis*, the incorporation of certain mutant DNA sequences into telomeres leads to uncapping of telomeres, manifested by dramatic telomere elongation and increased length heterogeneity (telomere deregulation). Here we show that telomere deregulation leads to enlarged, misshapen “monster” cells with increased DNA content and apparent defects in cell division.

However, such deregulated telomeres became stabilized at their elongated lengths upon addition of only a few functionally wild-type telomeric repeats to their ends, after which the frequency of monster cells decreased to wild-type levels. These results provide evidence for the importance of the most terminal repeats at the telomere in maintaining the cap complex essential for normal telomere function. Analysis of uncapped and capped telomeres also show that it is the deregulation resulting from telomere uncapping, rather than excessive telomere length per se, that is associated with DNA aberrations and morphological defects.

Key words: telomere • telomerase • chromosome aberrations • cell division • *Kluyveromyces lactis*

TELOMERES function to protect chromosomes from incomplete replication (Watson, 1972; Olovnikov, 1973), end-to-end fusions (McClintock, 1941; van Steensel et al., 1998), and loss (Kyrion et al., 1992; Sandell and Zakian, 1993). The G-rich strand of telomeric DNA is templated and synthesized by the cellular ribonucleoprotein telomerase (Greider, 1995). Telomeric DNA is bound by proteins, forming a chromosome-protective cap (reviewed in Grunstein, 1997). It was shown previously that mutation of the *Tetrahymena thermophila* telomerase RNA gene (*TER*) results in the addition of mutant telomeric DNA to the chromosome termini, and dramatic cellular phenotypes (Yu et al., 1990; Lee et al., 1993; Romero and Blackburn, 1995). These include blockage of cells in late anaphase with failed chromosomal separation and somatic nuclei containing much greater than normal DNA content (Yu et al., 1990; Lee et al., 1993), suggesting that proper telomere function is important for completing nuclear division and mitosis (Kirk et al., 1997). Cells lacking either the *TER* gene or telomerase activity experience progressive telomere shortening with each cell division

(Lundblad and Szostak, 1989; Counter et al., 1992; Singer and Gottschling, 1994; McEachern and Blackburn, 1995; Bodnar et al., 1998) until telomeric DNA is reduced below a critical length, resulting in chromosome instability and failure of cells to proliferate. These results highlight the requirement for both the presence of telomeres and a minimal telomere length in order to form a functional telomeric cap complex.

In most species, including budding yeasts, telomere length is normally maintained within a narrow size range that is species specific (Walmsley and Petes, 1985; Henderson and Petes, 1992). Although the telomeric “set length” within a yeast strain may be affected by temperature (McEachern and Hicks, 1993), carbon-source, or growth conditions (Blackburn, E.H., unpublished results), length regulation is a robust process that keeps the length of a given telomere within a relatively homogenous, tightly regulated range. In the budding yeasts *Saccharomyces cerevisiae* and *Kluyveromyces lactis*, telomere length has been experimentally manipulated by mutation of either telomeric DNA itself (via mutagenesis of the telomerase RNA gene template sequence), the telomerase enzyme, or the protein factors associated with the telomere (Prescott and Blackburn, 1997; Roy et al., 1999). In budding yeasts, the repressor–activator protein (Rap1p) binds duplex telomeric DNA repeats (Berman et al., 1986; Buchman et al.,

Address correspondence to Elizabeth H. Blackburn, University of California, Department of Microbiology & Immunology, Box 0414, 513 Parnassus Avenue, San Francisco, CA 94143-0414. Tel.: (415) 476-7284. Fax: (415) 476-8201. E-mail: michair@itsa.ucsf.edu

1988). Alleles of *RAP1* with alterations in its COOH-terminal domain (*rap1'*) or its interacting factors, *RIF1* and *RIF2*, can have large effects on telomere set length and the ability of cells to tightly regulate telomere size at any length, resulting in increased length heterogeneity in the telomere population (Hardy et al., 1992; Kyrion et al., 1992; Wotton and Shore, 1997). Coincident with these telomeric alterations, *rap1'* strains can experience a 20–30-fold increase in the frequency of chromosome loss (Kyrion et al., 1992). Mutations in analogous Myb-like DNA binding proteins that interact with telomeric DNA in other species also affect telomere set length and heterogeneity, as well as chromosome stability (Broccoli et al., 1997; Cooper et al., 1997; van Steensel et al., 1998).

We chose to study the effects of telomere uncapping in *K. lactis* because of its advantages as a model system for studying telomere-related processes. Unlike *S. cerevisiae*, which has irregular repeats (Shampay et al., 1984), the *K. lactis* telomeric repeat is a 25-bp sequence that is copied precisely into telomeres (McEachern and Blackburn, 1994, 1995). This allows for the reliable incorporation of restriction sites into the telomere and hence the ability to follow such individual, marked mutant repeats in telomeres over many generations. In addition, *K. lactis* lacks the chromosome-internal telomeric repeat tracts that, in *S. cerevisiae*, can recombine with telomeres (Lundblad and Blackburn, 1993; Walmsley et al., 1984), making it problematic to track the origin of telomeric repeats appearing at the chromosome ends. However, 11 of *K. lactis*' 12 telomeres share subtelomeric homology and can recombine with one another, giving mutations incorporated into one telomere the potential to spread into the majority of the chromosome ends. In *K. lactis*, mutating the telomeric DNA, both within and outside of the Rap1p binding consensus sequence (see Fig. 1 a), can result in two distinct types of changes at telomeres: the telomeres quickly elongate and show greatly increased length heterogeneity (deregulation). Such telomere deregulation has been attributed to disruption of the cap complex and consequent loss of end protection (Krauskopf and Blackburn, 1996, 1998). The *ter1-Acc* mutation in the *K. lactis* telomerase RNA template disrupts Rap1p binding in vitro and results in immediate, dramatic telomere lengthening within 50 generations of introduction of the *ter1-Acc* gene (McEachern and Blackburn, 1995). These telomeres are also highly deregulated, as judged by their massive length heterogeneity in Southern blot analyses, manifested as a smear of fragments ranging in size from smaller than wild-type (250–500 bp) to many kilobases (≥ 25). This degree of lengthening implies that >500 bp of telomeric DNA was added per cell division in the *ter1-Acc* strain, compared with the normal average of 5 bp required to maintain stable telomeric DNA length in wild-type yeasts (Singer and Gottschling, 1994; McEachern and Blackburn, 1995). Two other mutations, *ter1-Bgl* and *ter1-Kpn*, cause the telomeres to remain short and regulated for many generations, and then to abruptly elongate and deregulate much like *ter1-Acc* (McEachern and Blackburn, 1995). This telomere deregulation and elongation occurs only many generations (>750) after the introduction of the mutant *ter1* gene. Interestingly, the *ter1-Bgl* and *ter1-Kpn* mutations are located outside the telomeric Rap1p consensus binding site,

and do not affect in vitro Rap1p binding affinity (Krauskopf and Blackburn, 1996).

Previous studies of the *ter1-Acc*, *ter1-Bgl*, and *ter1-Kpn* *K. lactis* mutants have focused on their kinetics of telomere uncapping and elongation as well as their effects on telomere cap-prevented recombination (McEachern and Blackburn, 1994, 1995). Here, using these same mutants, we analyze how the telomere deregulation and elongation resulting from telomere uncapping affects both cell populations and individual cells. In addition, we specifically addressed whether it is the mean length of telomeres, or the cell's ability to regulate telomere length, that is important for cell viability. Previous results have provided evidence that the distal repeats of the telomere are especially important in end protection. *K. lactis* strains containing either the *ter1-AA*, *ter1-Bsi*, or *ter1-Kpn* template mutant genes in combination with a COOH-terminally deleted *RAP1* allele experience rapid telomere elongation and colony inviability like that in the *Acc* mutant (Krauskopf and Blackburn, 1996, 1998). Addition of wild-type repeats to the *ter1-AA* mutant telomeric termini (recapping) converts the telomeric DNA from an unregulated smear to a regulated pattern of discrete bands when visualized by Southern blot analysis. We similarly recapped *Acc*, *Bgl*, and *Kpn* strains with a phenotypically silent marked telomeric repeat to investigate how a wild-type-like distal end affects these mutant telomeres and the cellular phenotypes.

We report here that the deleterious effects of the *ter1-Acc*, *ter1-Bgl*, and *ter1-Kpn* mutations are distinct from those in senescing cells lacking the *TER1* gene, and are completely reversed by the addition of a functionally wild-type cap to the terminal mutant telomeric repeats. We conclude that the observed cellular phenotypes of these mutant strains are caused by the telomere deregulation resulting from cap complex disruption and subsequent loss of end protection, rather than extreme telomere elongation.

Materials and Methods

Strains

All *K. lactis* haploid strains were derived from the parental haploid strain K7B520 that has been previously described (McEachern and Blackburn, 1995). K7B520 was transformed with up to 10–50 ng/ μ l of pTER-BX plasmid, a YIP5 derivative containing the wild-type *TER1* gene with described template mutations (Fig. 1 a). Cells were electroporated (1.5 kV, 200 Ω , 25 μ F) and plated on medium lacking uracil and containing 1 M sorbitol. After 2 d, transformants were restreaked onto 5-fluoroorotic acid-containing medium and resistant colonies were screened for the desired gene replacement by digestion of PCR products with the restriction enzyme whose site was formed in the mutated template. PCR primers used were: upper strand, 5' GTC AAG TTC TGG AGG and lower strand, 5' CGA AGA GAA GAA TGG (GIBCO BRL). Cells were passaged by restreaking representative colonies onto yeast extract/peptone/dextrose and grown for 3 d at 30°C.

Southern Blotting Analyses

Genomic DNA was prepared from cells grown in yeast extract/peptone/dextrose at 30°C until late log phase. At least three independent isolates were cultured for each of the uncapped *ter1-Acc*, *ter1-Bgl*, and *ter1-Kpn* strains. At least three independent loop-outs were cultured for *ter1-Bcl* recapped and Δ *ter1* strains. DNA was cut with *EcoRI* (New England Biolabs Inc.) and the appropriate second restriction enzyme at 37°C overnight

(47°C for *Bcl*) and electrophoresed 0.8% agarose, 1× TBE gels at 40 V for 24 h or 1% 0.5× TBE pulsed-field gels at 230 V for 16 h (50 ms pulse time). After depurination, samples were transferred to Hybond N⁺ nitrocellulose (Amersham Corp.) and cross-linked with 1200 μJ using a Stratalinker 1800 (Stratagene Inc.). Hybridizations were carried out in 0.5 M Na₂HPO₄, 7% SDS, 0.5 mM EDTA at 50°C for 4–16 h and washed twice for 5 min at 40–50°C with 200 mM NaCl wash buffer. The wild-type (WT)¹ telomeric sequence probe used for all blots shown was 5' TAA TCA AAT CCG TAC ACC ACA TAC C. Blots were exposed to autoradiography film (Eastman-Kodak Co.) and scanned at 300 dots-per-inch resolution.

FACS[®] Analysis

Triplicate *K. lactis* cultures were grown to an A₆₀₀ of 0.5–1. Triplicate cultures from a single stock were used for each uncapped strain, while three independent loop-out strains were used for re-capped and *Δter1* strains. Cells were centrifuged at ~5,000 rpm in a clinical centrifuge and washed twice in 1 ml PBS. Washed cells were then fixed in 70% ethanol in PBS and diluted to 1 A₆₀₀ U/ml (~2 × 10⁷ cells/ml). A 1-ml sample of fixed cells was washed twice with 1 ml PBS. Cells were resuspended in 500 μl PBS + 1 mg/ml RNase A (QIAGEN Inc.) and incubated overnight on a rotating platform at 4°C. Afterwards, 20 μg of Proteinase K (Boehringer-Mannheim Biochemicals) was added and samples were incubated at 55°C for 1 h. Cells were centrifuged at 5,000 rpm in a microfuge, washed once with 1 ml of PBS, and resuspended in 500 μl of 50 μg/μl propidium iodide (Sigma Chemical Co.) for 1 h at room temperature in the dark. Stained samples were diluted 1:10 in PBS and 30,000 ungated events were counted at 650 nm wavelength on a FACS Calibur[®] (Becton Dickinson & Co.).

For statistical analyses, the mean of the 2 N peak was measured and the >2.5 N cutoff was calculated using gated plots for each sample. We arbitrarily chose “greater than diploid content” as exceeding 2.5 N. Statistical t-tests were performed using Microsoft Excel 98. Gated histograms were imported into Adobe Photoshop, where line thickness and gray shade were manipulated for overlays (see Fig. 3).

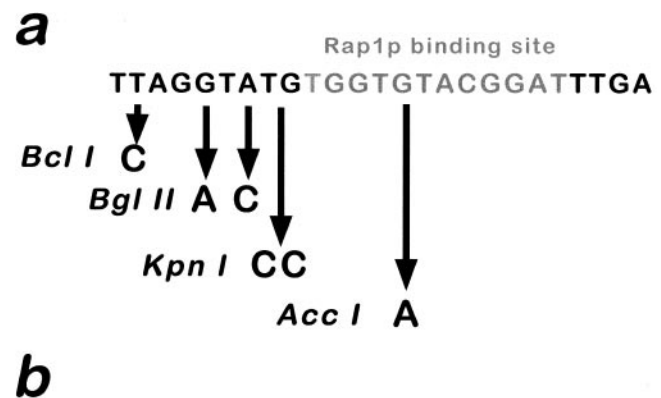
Microscopy

The same fixed samples used for FACS[®] analyses (see above) were used for microscopic analyses carried out in parallel. Approximately 1 ml of 70% ethanol/PBS-fixed cells was centrifuged at 5,000 rpm in a microfuge and washed twice with 500 μl of PBS. Cells were stained for 5–15 min at room temperature with 1 μg/ml 2,6-diamidinophenylindole (DAPI) and washed twice with 1 ml of PBS. At least three isolates of each strain were resuspended in 500 μl of PBS and sonicated for 10–30 s at 30% duty with a sonifier (Bransony Ultrasonics Corp.). Microscopy was performed using 2 μl of cells on a Microphot FXA microscope (Nikon Inc.) at 100× magnification and photographed onto 400 ISO film (Eastman-Kodak Co.). The *Δter1* image (see Fig. 4 b) was acquired on a DMLB microscope (Leica Inc.) with a 300 dpi color CCD camera. The total number of cells counted for each mutant is noted in Table I. Photographs were scanned at 300 dpi resolution and then cropped in Adobe Photoshop.

Results

DNA Analyses of Strains Containing Uncapped Telomeres

The telomeric DNA phenotypes of *ter1-Acc*, *ter1-Bgl*, and *ter1-Kpn* mutants have been reported previously (McEachern and Blackburn, 1995). For the present studies, these findings were confirmed using fresh cultures of the same strains and are summarized in Fig. 1 b. All three mutations resulted in dramatic telomere deregulation and elongation (Fig. 2 a, lanes 3, 9, and 15, and b, lanes 7, 13, and 20) compared with wild-type (Fig. 2 a, lane 1, and b, lane 1). We define deregulation as the smeary, heterogeneous population of telomeric DNA species identified on



Mutant	In vitro Rap1p Binding	Telomere Length	
		~150 gen.	>750 gen.
<i>Acc</i>	~ 1%	Long	Long
<i>Kpn</i>	Normal	Short	Long
<i>Bgl</i>	~ 200%	Short	Long
<i>Bcl</i>	Normal	WT	WT

Figure 1. The *TER1* template and mutants. (a) The *K. lactis* telomeric repeat sequence. Grey nucleotides represent the Rap1p binding site. Arrows indicate base mutations for *ter1* mutants, which are named by the unique restriction enzyme site they create in the repeat. (b) Summary of the in vitro Rap1p binding affinity as a percentage of wild-type and the associated telomere length phenotypes of *ter1* mutants. Short telomeres are any length shorter than WT. Long telomeres are longer than the longest WT telomere (~3.5 kb).

these Southern blots. The apparent sizes of the heterogeneous telomeres in these mutant strains ranged from less than the smallest wild-type telomeric restriction fragment to ≥25 kb. The elongated mutant DNA was largely made up of mutant telomeric DNA repeats, as shown by secondary digestion with each restriction enzyme whose site was copied into telomeric DNA by the mutant telomerase (Fig. 2 a, lanes 4, 10, and 16). After cleaving off the mutant repeats, the length of these secondarily digested telomeric fragments reflects the remaining length of the original WT repeat tract that is located internally to the added mutant repeats on the telomere (Fig. 2 c). The size ranges of these internal wild-type repeat tracts were generally similar in all the mutants studied (bracketed area in Fig. 2 a, lanes 1, 4, 7, 10, 13, and 16). While the range of internal telomere sizes in *ter1* template mutants was comparable to WT, the individual telomere lengths were slightly shorter than WT after the deregulation following uncapping (Fig. 2 a, compare lane 1 with 4, 10, and 16). In addition, the patterns were different from the WT patterns. This change in the patterns of telomeres has been shown previously to be due to the extensive subtelomeric recombination and has been documented in *ter1-Acc* and late passage *Bgl* and *Kpn* strains (McEachern and Blackburn, 1995). The 3.5-kb telomeric fragment that lacks subtelomeric homology to the other telomeres (cut by *AccI* in Fig. 2 a, lanes 4 and 5)

1. Abbreviations used in this paper: DAPI, 2,6-diamidinophenylindole; WT, wild-type.

those of $\Delta ter1$ survivors were quite short and formed discrete size classes that were regulated. Thus, these short $\Delta ter1$ telomeres were distinct from the degraded telomeric species observed in the three $ter1$ template mutant strains.

We used FACS[®] analysis to investigate the cellular DNA content of $ter1$ template mutant and $\Delta ter1$ cell populations (Fig. 3). In the WT *K. lactis* control strain, 13% of the cells contained DNA in excess of diploid content (Fig. 3 a, black histogram). Similarly, 10–16% of early passage (i.e., ~150 generation) $ter1-Bgl$ and $ter1-Kpn$ cells, which have short well-regulated telomeres (Fig. 2 b, lanes 10 and 17), had greater than diploid DNA content (data not shown). While presenescent $\Delta ter1$ cells had a DNA content profile similar to WT (data not shown), postsenescent $\Delta ter1$ survivor cultures with short, relatively homogeneous telomeres (Fig. 2 b, lane 6) exhibited a 27% subpopulation of cells with greater than diploid DNA content (Fig. 3 a, dashed histogram). Likewise, $ter1-Acc$ cells, and late passage (>750 generations) $ter1-Bgl$ and late $ter1-Kpn$ cells, which all had deregulated telomeres, showed 27, 35, and 19% subpopulations of cells with greater than diploid DNA content, respectively (Fig. 3, b and c, black histograms, and data not shown). While the *Acc* and late passage *Bgl* mutants were significantly different from WT (both $P < 0.01$), the variability of the WT slightly decreased the significance of the difference from the late passage *Kpn* mutant ($P = 0.06$). The increase in DNA content in the $ter1$ template sequence mutants and $\Delta ter1$ survivor strains reproducibly coincided with a decreased percentage of cells with 1 N DNA content (Fig. 3, compare 1 N peak in black histograms with gray histograms in a–c). These DNA content changes are unlikely to be explained by an increase in telomeric DNA alone, since the $\Delta ter1$ survivors had much less telomeric signal than the $ter1$ mutants but still exhibited an increased DNA content (Figs. 2 b, lane 6, and 3 a, dashed histogram). Furthermore, even assuming that all 12 telomeres in haploid *K. lactis* lengthened to an average of 100 kb, this would only represent approximately one tenth of the haploid genome size (Seoighe and Wolfe, 1998). Hence, the increased DNA content of these $ter1$ mutants was likely to have resulted from either endoreduplication and/or defects in chromosome segregation.

Microscopic Analyses of $ter1$ Mutants

To determine whether DNA segregation was affected in $ter1$ template sequence mutants, we used fluorescence light microscopy and DAPI staining to examine the cellular DNA, and brightfield microscopy to examine overall cell morphology and cell budding indices (Figs. 4–6, and Table I). We predicted that if DNA segregation were affected, then multiple or large DAPI-staining structures should be visible in a single cell body and some percentage of cells might contain little or no DNA. While WT and presenescent $\Delta ter1$ cells looked indistinguishable (Fig. 4 a and data not shown), postsenescent $\Delta ter1$ survivors had a 4% population of somewhat enlarged, misshapen cells with abnormally distributed DNA (Table I). These cells also had very degraded cell walls and collapsed buds, as judged by brightfield microscopy (Fig. 4 b, arrowheads).

We found that 10% of $ter1-Acc$ mutant cells had cellular

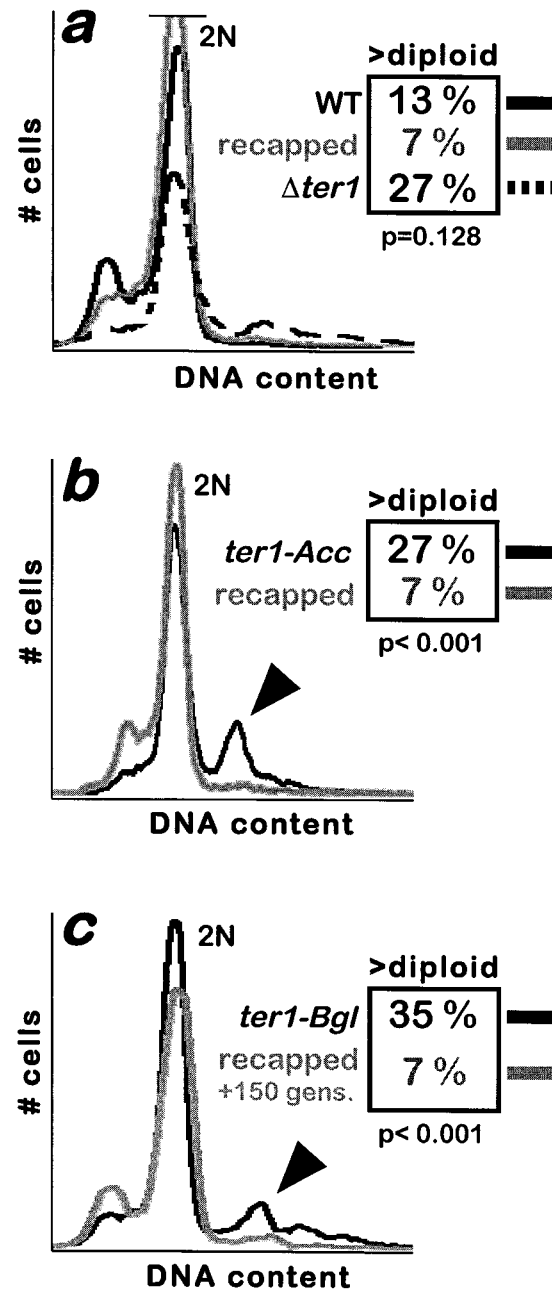


Figure 3. FACS[®] analysis of uncapped (black histogram) versus recapped (gray histogram) *TER1* and $\Delta ter1$ survivor (dashed histogram) strains (a), $ter1-Acc$ (b), and $ter1-Bgl$ >750 generation (c) strains. Representative plots show number of cells versus propidium iodide signal (>650 nm). 2 N peak is indicated. Relevant population percentages are shown as rounded averages of at least three replicates. Statistical P values are from t tests of data from uncapped versus recapped populations.

defects. These were distinctly different from, and more severe than, the most extreme morphological defects of postsenescent $\Delta ter1$ cells. Many $ter1-Acc$ mutant cells had multiple DAPI-staining structures (Fig. 4, d and e, arrows), while others had no brightly staining DAPI structures but did contain large areas of diffuse DAPI staining (data not shown, see similar phenotypes for *Bgl* and *Kpn*

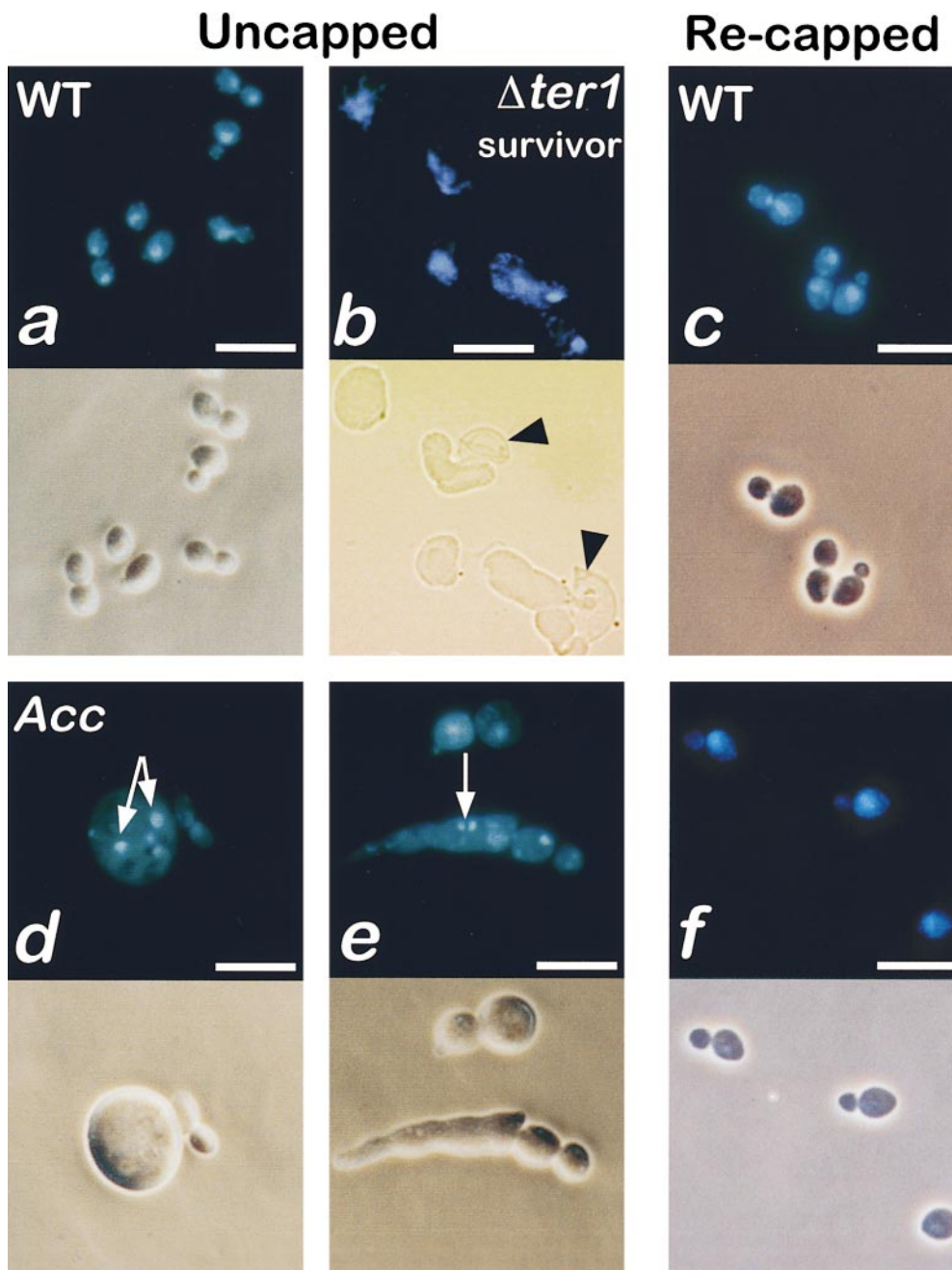


Figure 4. (a) DAPI (top) and brightfield (bottom) microscopy for wild-type *K. lactis* cells. (b) Postsenescent $\Delta ter1$ survivor strain. (c) Wild-type strains recapped with *ter1-Bcl*. (d and e) DAPI and brightfield microscopy showing representative *ter1-Acc* monster cells. Arrows, multiple large DAPI-staining structures within a cell body. (f) *ter1-Acc* cells recapped with *ter1-Bcl*. Bars: 10 μ M.

mutants in Figs. 5 d and 6 d). These *Acc* cells often appeared to have budding and division defects. They were frequently grossly enlarged or elongated (Fig. 4, d and e), and some cells formed chains that were resistant to extensive sonication (Fig. 4 e). Other cells were spherical but enlarged to up to five times the diameter of wild-type cells (Fig. 4 d). We use the term “monster cells” generally to describe these phenotypes, with a given cell needing only to exhibit one of these traits to qualify as a monster cell.

The *ter1-Bgl* and *ter1-Kpn* mutations also resulted in monster cell phenotypes, but only in cell populations with deregulated, elongated telomeres. Thus, early passage (~150 generations) *ter1-Bgl* and *ter1-Kpn* strains with short, regulated telomeres showed no significant monster

cell phenotypes above background levels (Figs. 5 a and 6 a), while isogenic isolates passaged for >750 generations and, with deregulated telomeres, exhibited high levels of severe monster cell phenotypes. The percentages of monster cells in the populations of late passage *ter1-Bgl* and *ter1-Kpn* cell strains were 12 and 13%, respectively (Table I). The same monster cell populations also contained either multiple DAPI-staining structures (Figs. 5 c and 6, c and d, arrows) or decondensed DAPI-staining material (Figs. 5 d and 6 d, arrowheads) and apparent budding and division defects similar to the *ter1-Acc* mutant cells (Figs. 4 e, 5 c, and 6 c).

Our microscopic analyses highlight the differences between the abnormal phenotypes associated with senes-

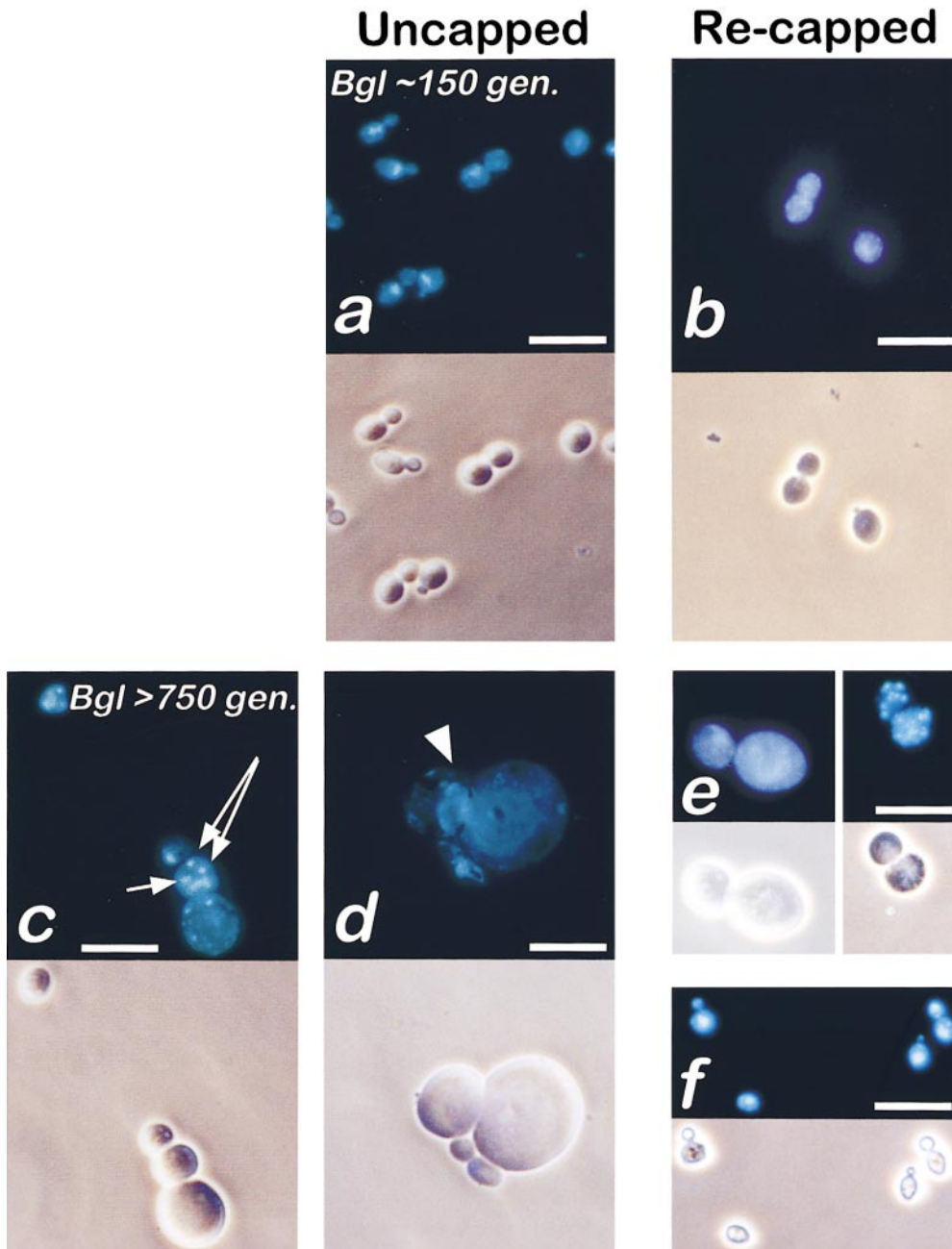


Figure 5. (a and b) DAPI (top) and brightfield (bottom) microscopy for uncapped versus recapped, early passage (~150 generation) *ter1-Bgl* cells. (c and d) DAPI and brightfield microscopy for representative late passage (>750 generation) *ter1-Bgl* monster cells. Arrows, large multiple DAPI-staining structures within a single cell body. Arrowhead, decondensed, enlarged nuclear material. (e and f) *ter1-Bgl* late passage cells recapped with *ter1-Bcl* immediately (e) and ~150 generations after (f) recapping. Bars: 10 μ M.

cence and monster cells. Although postsenescent $\Delta ter1$ survivors were phenotypically abnormal, they had irregular, degraded cell walls and collapsed buds unlike those of the *ter1* template sequence mutants. Furthermore, postsenescent $\Delta ter1$ survivors did not exhibit multiple DAPI-staining structures within one cell. Finally, the incidence of monster cells in postsenescent $\Delta ter1$ populations was at most a third that of other *ter1* strains and was considerably more variable between lineages (Table I). In summary, we concluded that telomere uncapping was caused by the *Acc*, *Bgl*, or *Kpn* mutations and resulted in telomere deregulation and elongation. This correlated with a subpopulation of cells containing DNA in excess of diploid amounts and a significantly increased percentage of morphologically aberrant monster cells that were distinct from postsenes-

cent $\Delta ter1$ survivors. The multiple DAPI-staining structures in all three uncapped *ter1* template mutant strains suggested that the cell's ability to segregate DNA was inversely correlated with the extent of telomere deregulation/elongation.

Telomere Recapping Restores Length Regulation

We wished to dissect which property of the uncapped telomeres caused the extreme monster phenotypes described above: deregulation or extreme length. To address this issue, we replaced the mutant *ter1* gene in *Acc*, *Bgl*, and *Kpn* strains with a *ter1-Bcl* allele, which adds phenotypically silent, functionally wild-type, repeats to the telomeric DNA end (McEachern, M.J., and E.H. Blackburn, unpublished

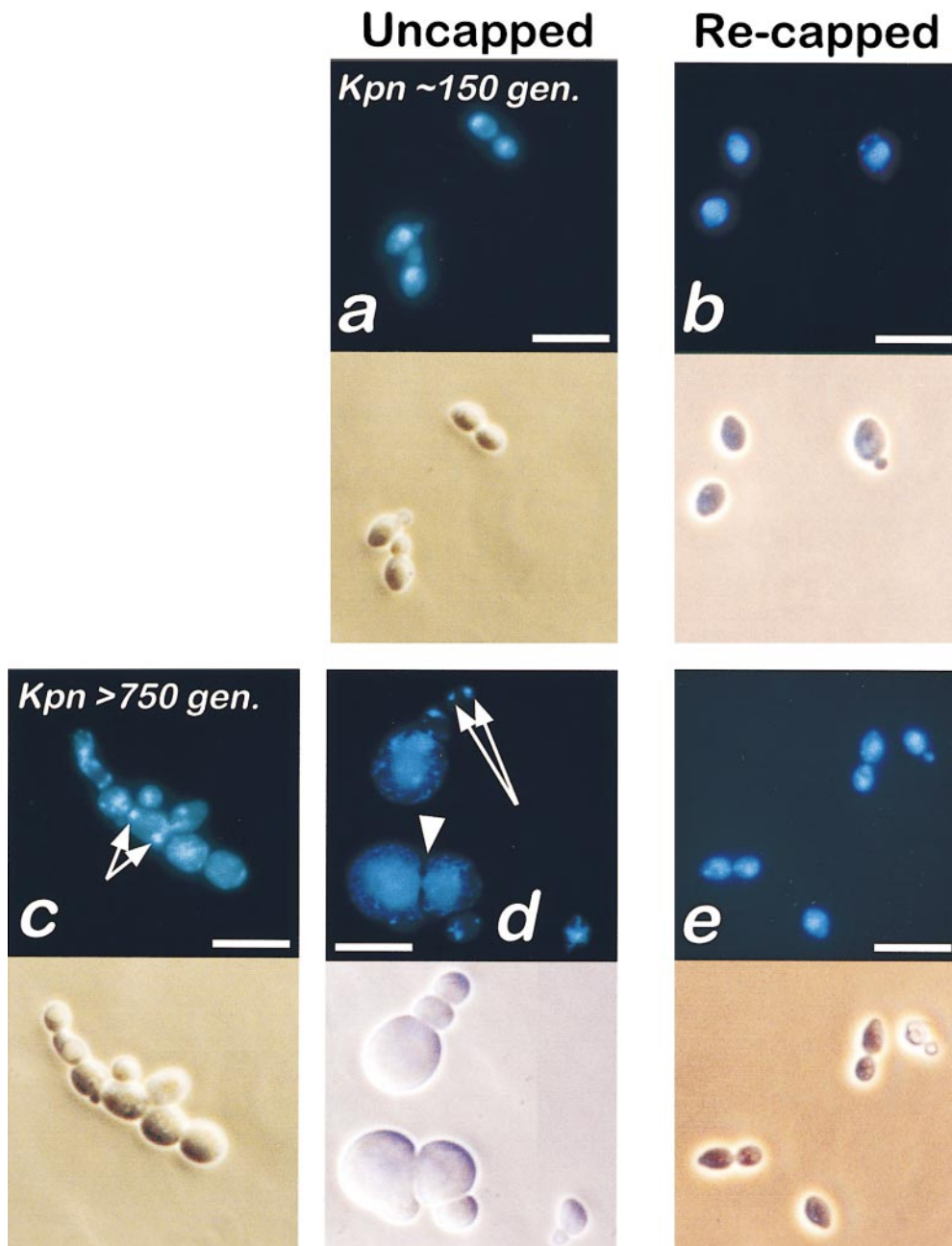


Figure 6. (a and b) DAPI (top) and brightfield (bottom) microscopy for uncapped (a) versus recapped (b), early passage (~150 generation) *ter1-Kpn* cells. (c and d) DAPI and brightfield microscopy for representative late passage (>750 generation) *ter1-Kpn* monster cells. Arrows, large multiple DAPI-staining structures within a single cell body. Arrowhead, decondensed, enlarged nuclear material. (e) *ter1-Kpn* late passage cells recapped with *ter1-Bcl*. Bars: 10 μ M.

results; Krauskopf and Blackburn, 1998; Roy et al., 1999). The *Bcl* repeats contain a *BclI* restriction enzyme site, so that these added marked repeats can be distinguished from preexisting wild-type or other mutant repeats. The *Bcl* repeats bind Rap1p normally in vitro and thus were predicted to allow the previously disrupted telomere cap to reform at the distal end of the telomere. In all three mutant *ter1* strains studied, recapping with *Bcl* repeats caused a transition from a deregulated smear of telomeric DNA to a series of discrete, length-regulated but still elongated telomeric bands (Fig. 2 b, arrows, compare lanes 7 with 8, 13 with 14, and 20 with 21). This transition occurred within ~50 generations (the earliest time point at which DNA could be analyzed). These reregulated telomeres remained much longer than wild-type (Fig. 2 b, lanes 8, 14, and 21),

with a significant fraction of the telomere signal still at limit mobility (≥ 25 kb) for the *Bgl* and *Kpn* mutants (Fig. 2 b, lanes 14 and 21). Recapping did not significantly change the sizes of the internal wild-type repeat tracts (Fig. 2 a, compare lanes 4 with 5, 7 with 8, 10 with 11, 13 with 14, and 16 with 17). Digestion of the cap repeats with *BclI* revealed that only three to four *ter1-Bcl* repeats were added to each telomere (Fig. 2 b, compare lanes 8 with 9 and 21 with 22). Interestingly, in late *ter1-Bgl* cells, the *Bcl* repeats seemed to incorporate further into some late passage telomeres, since digestion of the cap resulted in large decreases in the sizes of some telomere restriction fragments (Fig. 2 b, compare lane 14 with 15). The inward migration of these repeats may have been due to faster terminal repeat turnover (Krauskopf and Blackburn, 1998)

Table I. *TER1* and *ter1* Budding Indices

	Unbudded	Small budded	Large budded	Monster	No. cells
WT	22 ± 7	32 ± 2	46 ± 8	0	1,555
recapped	19 ± 1	29 ± 0.6	52 ± 0.5	0.3 ± 0.6	299
<i>Δter1</i> survivor	11 ± 4	28 ± 3	57 ± 2	4 ± 3	529
<i>ter1-Acc</i>	15 ± 0.9	18 ± 0.7	57 ± 0.1	10 ± 0.1	701
recapped	23 ± 2	29 ± 5	47 ± 3	0	301
<i>ter1-Bgl</i>					
~150 gen	18 ± 3	29 ± 3	49 ± 3	3 ± 0.7	709
recapped	14 ± 0.7	33 ± 1	52 ± 1	0.3 ± 0.5	308
>750 gen	16 ± 4	21 ± 0.4	51 ± 4	12 ± 1	703
recapped	8 ± 2	29 ± 2	54 ± 2	9 ± 0.5	302
recapped +150 gen	27 ± 3	28 ± 3	44 ± 2	0.9 ± 0.8	1,153
<i>ter1-Kpn</i>					
~150 gen	18 ± 2	27 ± 2	53 ± 2	3 ± 0.2	708
recapped	16 ± 3	30 ± 0.4	53 ± 2	0.7 ± 0.6	304
>750 gen	14 ± 2	20 ± 0.9	53 ± 2	13 ± 0.9	943
recapped	21 ± 1	28 ± 2	51 ± 0.8	0.7 ± 0.6	302

Budding indices of wild-type and *ter1 K. lactis* strains. Standard deviations are shown. Monster cell populations are in bolded text. gen, generations.

or recombination, since isogenic cells passaged for an additional 150 generations exhibited a significantly altered telomere pattern (Fig. 2 b, compare lane 15 with 16).

To determine whether telomeric DNA shortened overall after recapping with *Bcl* repeats, we performed quantitative analyses of the total telomeric hybridization signal in uncapped and recapped lanes, for all three *ter1* template mutants (Fig. 2 b and data not shown). We repeated these analyses using pulse-field gel electrophoresis and compared the total telomeric signals on four chromosomes between uncapped and recapped strains (data not shown). In all cases, there was no significant decrease in telomeric signal after recapping.

In summary, the internal WT repeat tracts of uncapped telomeres in *ter1* template mutants shortened only slightly, and were longer than those in postsenescent *Δter1* survivors. Recapping added an average of three to four *ter1-Bcl* repeats to the distal tips of telomeres, although in some cases recombination events allowed migration of *Bcl* repeats further into the telomere. In all cases, however, the recapped *ter1* strains regained their ability to regulate telomere length about a new mean size, and the majority of telomeres remained significantly elongated.

Telomere Recapping Restores Normal Cellular Phenotypes in Mutant *ter1* Strains

The recapped *ter1* template mutant strains were examined by FACS[®] analysis (Fig. 3). After recapping, all three *ter1* strains eventually exhibited significantly fewer cells with greater than diploid DNA content. The percentage of recapped *ter1-Acc* and *ter1-Bgl* cells with greater than diploid DNA content was the same (7%) as in recapped wild-type cells (Fig. 3, a–c, gray histograms). Interestingly, in *ter1-Bgl* strains, DNA content did not show an immediate large decrease upon recapping (data not shown). However, ~150 generations after recapping, the fraction of cells with greater than diploid DNA content was reduced to wild-type levels (Fig. 3 c, gray histogram). In contrast, recapped late passage *ter1-Kpn* strains showed a significant decrease in cells with greater than diploid DNA con-

tent as soon as cells could be analyzed (from 19 to 9%; $P < 0.001$, data not shown).

By the criteria of DAPI staining and brightfield microscopic analyses, the nuclear and cell morphologies of recapped *ter1-Acc* and late passage *ter1-Kpn* strains were indistinguishable from wild-type (Figs. 4 f and 6 e, and Table I), even though their telomeres remained very long. The early passage recapped *ter1-Bgl* and *ter1-Kpn* strains also had DNA contents and percentages of monster cells comparable to wild-type (data not shown, Figs. 5 b and 6 b, and Table I). Immediately after recapping, the late passage *ter1-Bgl* strain still exhibited a 9% subpopulation of monster cells (Table I). Qualitatively, these recapped *ter1-Bgl* cells were not as large or grotesquely malformed as the uncapped *ter1-Bgl* monster cells (Fig. 5, compare c and d with e). However, ~150 generations after recapping, the percentage of monster cells returned to wild-type levels (Fig. 5 f, and Table I) even though the telomeres in these cells appeared qualitatively similar to those immediately after recapping (Fig. 2 b, compare lanes 15 with 16). Thus, while Southern blot analyses showed that *ter1-Bcl* repeats had been physically added to the distal ends of telomeres within 50 generations, it took additional time for late passage *ter1-Bgl* mutants to establish a cell population with functional telomeric caps.

Discussion

The DNA–protein complex at the end of telomeres is thought to be important for their chromosome-protective functions. When this distal cap complex is disrupted by adding mutant repeats or shortening the existing telomere beyond a critical length, the chromosome becomes uncapped and subject to damage. Uncapping can be defined as the loss of end protection and results in either net telomere shortening or lengthening, increased recombination in telomeric regions, and/or the loss of regulation about a mean telomere length. Here we have addressed two questions related to telomere length regulation in *K. lactis*. First, what are the cellular phenotypic consequences of uncapped telomeres in *ter1* template sequence mutants and

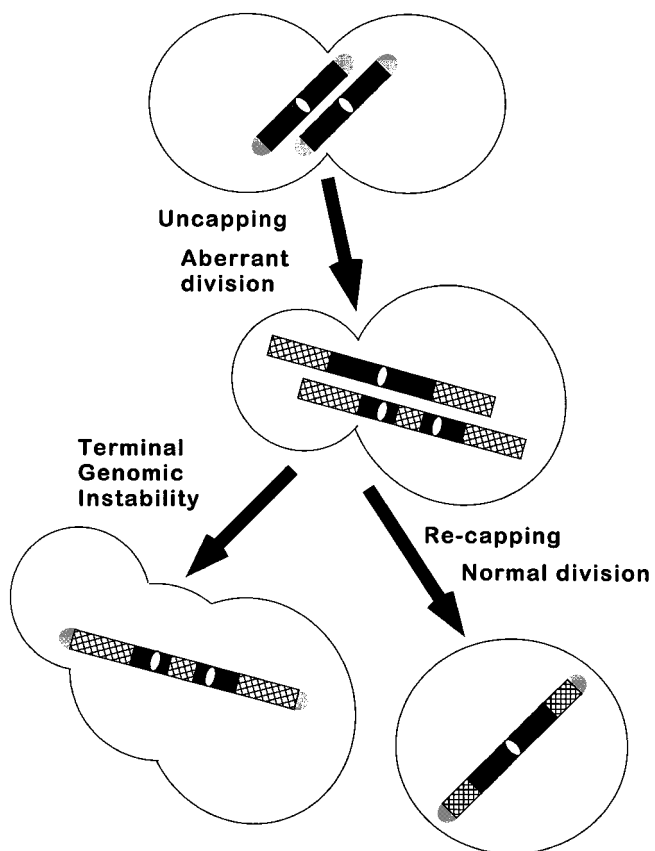


Figure 7. Model for monster cell formation and effects of recapping. (Top) A large budded haploid cell ready for mitosis. One pair of sister chromatids shown. (Middle) Uncapping leads to chromosome aberrations such as dicentric chromosomes (lower chromosome). (Bottom left) Segregation of damaged chromosomes leads to terminal monster cells. (Bottom right) Recapping of strains with stable chromosomes allows normal division to occur.

postsenescent $\Delta ter1$ survivor strains? Second, upon finding that cells respond poorly to telomere uncapping, we asked whether it is the resulting telomere deregulation, as opposed to elongation per se, that is correlated with the observed phenotypes.

This is the first detailed report in yeast of the cellular morphological consequences caused by telomere uncapping. Telomere uncapping in *ter1* template sequence mutants was correlated with a greater than diploid DNA content, aberrant nuclear morphologies, and apparent cell division defects. We conclude that it is the deregulation of telomeres resulting from uncapping, rather than their elongation, that is associated with these phenotypes. The addition of a few wild-type-like repeats to the extreme terminus of the elongated mutant *ter1* telomeres allowed strains to regain their ability to regulate telomeres, even though the telomeres were up to $100\times$ longer than wild type. Interestingly, the *ter1-Bgl* mutant telomeres were not fully capped at first and *Bcl* repeats migrated further into the telomeres than in other mutants. This may have been due to continued degradative shortening of the telomeres followed by de novo *Bcl* addition or recombination of the

Bcl cap with the internal tracts. However, after being re-capped for ~ 150 generations, *Bgl* mutant strains behaved similarly to the *Acc* and *Kpn* mutants. Hence, telomere re-capping eventually caused the DNA content and cellular morphology to return to normal in all three *ter1* mutants.

The mechanism by which the deregulation of uncapped telomeres leads to monster cell formation in *K. lactis* is not known. While general genomic instability and consequent misregulation of gene expression may result in monster cells, the addition of a wild-type telomeric cap is sufficient for recovery of the cell population. In *S. cerevisiae*, senescing cells show increased chromosome loss (Lundblad and Szostak, 1989). Likewise, elongated, poorly regulated telomeres can increase chromosome loss rates (Kyrion et al., 1992). Telomere uncapping can lead to either telomere shortening ($\Delta ter1$) or deregulation/elongation (*ter1* template mutants); we have shown here that each has distinct telomere and monster cell phenotypes. The $\Delta ter1$ survivors had cell walls that appeared degraded and they did not show multiple DAPI-staining structures in one cell body. On the other hand, monster cells of *ter1* template sequence mutants had healthy-looking cell walls, decondensed chromatin, often up to 10 nucleus-sized DAPI-staining objects in a single cell body, with frequently no DNA in the adjacent body. Evidence supporting DNA segregation or replication defects includes the observation that the DNA content of cultures with elongated, uncapped telomeres was greatly increased. Taken together with the observation of cells with either increased DAPI-staining or no staining and the morphological results, these results strongly suggest that deregulated telomeres can cause DNA missegregation.

A Model for the Effects of Deregulated, Uncapped Telomeres on Chromosome Segregation and Cell Morphology

We propose the following model for how uncapped telomeres may negatively affect cells (Fig. 7). While deletion of *ter1* results in telomere shortening until the cap is lost, addition of certain mutant repeats can disrupt the cap without telomere shortening. Mutant repeats that cannot bind Rap1p (i.e., *Acc*) result in immediate telomere uncapping, while mutant repeats that retain Rap1p binding (*Bgl* and *Kpn*) do not result in immediate uncapping. The effects of the *Bgl* and *Kpn* mutations accumulate over time (McEachern and Blackburn, 1995) until some as yet undefined change(s) in the properties of the Rap1p-nucleated complex on the mutant telomeric DNA prevents functional end protection. Uncapped telomeres may over elongate by telomerase-mediated or recombination pathways at this point (McEachern and Blackburn, 1996; Krauskopf and Blackburn, 1998). Such telomeres are also subject to degradation, as shown by the smear of telomeric signal migrating faster than wild-type telomeres (Fig. 2 b, lanes 7, 13, and 20). Uncapped, elongated telomeres may be recognized as damage, causing cell cycle delay or accidental repair/telomeric fusion, resulting in dicentric chromosome formation. Individual chromosomes or whole genomes may be lost or missegregated. This genomic instability results in further negative phenotypic consequences for the cell. Once polyploidy or aneuploidy occurs, strong selec-

tion pressures exist for the healthiest cells, suggesting why the majority of cells in a population are not visually aberrant. However, microcolony analyses of phenotypically wild-type *ter1-Acc* mutant cells revealed that they continually give rise to subpopulations of monster cells (data not shown).

Recapping reverses the phenotypic effects of telomere deregulation. Reestablishment of a functional cap may occur immediately for the population, as in the cases of the recapped *ter1-Acc* and *ter1-Kpn* strains, or be slower, as in the case of the late passage *ter1-Bgl* mutant. We propose that recapping involves reforming a stable DNA-protein complex at the telomere ends, preventing these chromosomes from becoming deregulated and exerting detrimental effects. Cells with stably capped telomeres are likely to have a substantial growth advantage, and once a *ter1* population is recapped the frequency of unstable monster cells decreases as healthy cells take over the population.

The Importance of the Distal Telomeric Repeats for Cap Formation

The addition of three to four *ter1-Bcl* repeats to the termini of the telomere was sufficient to eventually cap *ter1-Acc*, *Bgl*, and *Kpn* mutant telomeres. The relatively few *Bcl* repeats that migrated into the *Bgl* telomeres did not appear to have a significant effect on the eventual capping of these telomeres. The telomeres in these recapped strains contain three distinguishable, possibly functional domains: the remaining ~250–300-bp internal tract of original wild-type repeats most proximal to the centromere, the adjacent large tract of *Acc*, *Bgl*, or *Kpn* mutant repeats, which may exceed 25 kb in length, and the (usually) three to four functionally wild-type *ter1-Bcl* repeats at the very terminus of the telomere (Fig. 2 c). Whether the remaining internal wild-type repeats were necessary for the reestablishment of a normal cell population after recapping is unknown. Notably, the total telomeric DNA hybridization signal in elongated *ter1* mutants remained unchanged after recapping, providing evidence that recapping is not obligatorily associated with a reduction in mean telomere length. This evidence strongly suggests that it is not telomere length, but the very terminal repeats that are important for preventing monster cell formation.

It is thought that functionally wild-type telomeres assume a higher-order structure nucleated on Rap1p that protects the chromosome end. The COOH terminus of Rap1p interacts with the Sir (Moretti et al., 1994) and Rif 1 and 2 (Wotton and Shore, 1997) proteins. Generally, mutations that prevent Rap1p interaction with telomeric DNA (i.e., template mutations), Sirs, and/or Rifs, or COOH-terminal mutations in Rap1p, result in telomere elongation, suggesting that these interactions help stabilize the telomeric complex that regulates telomere length (Kyriou et al., 1992; Krauskopf and Blackburn, 1996). The results reported here also address whether the monster cell phenotypes observed are the pleiotropic effects of changing the amounts of Rap1p or associated factors in the cell. In the case of the *Acc* mutation, Rap1p binds with significantly lowered affinity in vitro (Krauskopf and Blackburn, 1996), and, therefore, Rap1p occupancy of

these repeats in vivo may be low. Although 100-fold less Rap1p is predicted to bind *Acc* repeats, up to 100× as many repeats may be present at each telomere in *ter1-Acc* strains. Therefore, the overall Rap1p levels at telomeres may not differ greatly between wild-type and *ter1-Acc* cells. Nevertheless, the structure of their telomeric complexes are likely distinct. In contrast, both *Bgl* and *Kpn* mutant repeats have normal Rap1p binding affinity in vitro and upon elongation could potentially titrate Rap1p, along with interacting proteins, away from the scores of genes they regulate. Yet the functionally recapped *ter1-Acc*, *ter1-Bgl*, and *ter1-Kpn* strains all have as much telomeric DNA as uncapped strains and appear as healthy as wild type. Therefore, it is unlikely that titration of Rap1p explains the phenotypes associated with monster cells.

It is possible that the uncapped *ter1* mutants are unable to regulate the single-stranded ends of the telomere and are therefore unable to regulate length. The *Acc*, *Bgl*, and *Kpn* mutations may affect the interaction of putative end-binding factors, such as *K. lactis* homologues of the Cdc13p, Est1p, or Stn1p proteins found in *S. cerevisiae* (Nugent et al., 1996; Virta-Pearlman et al., 1996; Grandin et al., 1997). If these *ter1* mutant repeats were incapable of binding such end factors normally, this could expose the terminal region of the telomere to factors such as recombination-associated activities, including degradation enzymes.

A functional cap complex at the telomere ends appears to be important in other organisms besides budding yeasts. Mutations in the mammalian telomere binding proteins TRF1 and TRF2 have been shown to result in varying degrees of telomere lengthening and chromosome fusions, respectively (Bianchi et al., 1997; van Steensel et al., 1998). In *Schizosaccharomyces pombe*, the telomere binding protein Taz1p has been shown to be important in telomere length control (Cooper et al., 1997). Additionally, mutations in Taz1p that result in improper meiotic segregation, defects in telomere clustering, and low spore viability may reflect failure to form a functional cap (Cooper et al., 1998; Nimmo et al., 1998). Understanding the role of capping in telomere function will likely be useful in understanding the roles of telomeres in cell viability and division control.

We thank Mike McEachern for his generous gift of uncapped mutant *ter1* template sequence strains, the pTER-BX capping plasmid, and sharing unpublished results, and Anat Krauskopf and Mike McEachern for many fruitful discussions. We also thank Simon Chan, Sandy Johnson, Andrew Murray, and Thea Tlsty for critical review of the manuscript, Andrew Murray's lab for use of their microscope, and Rudi Grosschedl's lab for use of their FacsCalibur®.

This work was funded by National Institutes of Health (NIH) grants GM26259 to E.H. Blackburn, a National Science Foundation Graduate Fellowship to C.D. Smith and NIH training grant T32CA09270.

Received for publication 25 September 1998 and in revised form 4 March 1999.

References

- Berman, J., C.Y. Tachibana, and B.K. Tye. 1986. Identification of a telomere-binding activity from yeast. *Proc. Natl. Acad. Sci. USA* 83:3713–3717.
- Bianchi, A., S. Smith, L. Chong, P. Elias, and T. de Lange. 1997. TRF1 is a dimer and bends telomeric DNA. *EMBO (Eur. Mol. Biol. Organ.) J.* 16: 1785–1794.
- Bodnar, A.G., M. Ouellette, M. Frolkis, S.E. Holt, C.P. Chiu, G.B. Morin, C.B.

- Harley, J.W. Shay, S. Lichtsteiner, and W.E. Wright. 1998. Extension of lifespan by introduction of telomerase into normal human cells. *Science*. 279:349–352.
- Broccoli, D., A. Smogorzewska, L. Chong, and T. de Lange. 1997. Human telomeres contain two distinct Myb-related proteins, TRF1 and TRF2. *Nat. Genet.* 17:231–235.
- Buchman, A.R., W.J. Kimmerly, J. Rine, and R.D. Kornberg. 1988. Two DNA-binding factors recognize specific sequences at silencers, upstream activating sequences, autonomously replicating sequences, and telomeres in *Saccharomyces cerevisiae*. *Mol. Cell. Biol.* 8:210–225.
- Cooper, J.P., E.R. Nimmo, R.C. Allshire, and T.R. Cech. 1997. Regulation of telomere length and function by a Myb-domain protein in fission yeast. *Nature*. 385:744–747.
- Cooper, J.P., Y. Watanabe, and P. Nurse. 1998. Fission yeast Taz1 protein is required for meiotic telomere clustering and recombination. *Nature*. 392:828–831.
- Counter, C.M., A.A. Avilion, C.E. LeFeuvre, N.G. Stewart, C.W. Greider, C.B. Harley, and S. Bacchetti. 1992. Telomere shortening associated with chromosome instability is arrested in immortal cells which express telomerase activity. *EMBO (Eur. Mol. Biol. Organ.) J.* 11:1921–1929.
- Grandin, N., S.I. Reed, and M. Charbonneau. 1997. Stn1, a new *Saccharomyces cerevisiae* protein, is implicated in telomere size regulation in association with Cdc13. *Genes Dev.* 11:512–527.
- Greider, C.W. 1995. Telomerase biochemistry and regulation. In *Telomeres*. E.H. Blackburn and C.W. Greider, editors. Cold Spring Harbor Laboratory Press, Cold Spring Harbor, NY. 35–68.
- Grunstein, M. 1997. Molecular model for telomeric heterochromatin in yeast. *Curr. Opin. Cell Biol.* 9:383–387.
- Hardy, C.F., L. Sussel, and D. Shore. 1992. A RAP1-interacting protein involved in transcriptional silencing and telomere length regulation. *Genes Dev.* 6:801–814.
- Henderson, S.T., and T.D. Petes. 1992. Instability of simple sequence DNA in *Saccharomyces cerevisiae*. *Mol. Cell. Biol.* 12:2749–2757.
- Kirk, K.E., B.P. Harmon, I.K. Reichardt, J.W. Sedat, and E.H. Blackburn. 1997. Block in anaphase chromosome separation caused by a telomerase template mutation. *Science*. 275:1478–1481.
- Krauskopf, A., and E.H. Blackburn. 1996. Control of telomere growth by interactions of RAP1 with the most distal telomeric repeats. *Nature*. 383:354–357.
- Krauskopf, A., and E.H. Blackburn. 1998. Rap1 protein regulates telomere turnover in yeast. *Proc. Natl. Acad. Sci. USA*. 95:12486–12491.
- Kyriou, G., K.A. Boakye, and A.J. Lustig. 1992. C-terminal truncation of RAP1 results in the deregulation of telomere size, stability, and function in *Saccharomyces cerevisiae*. *Mol. Cell. Biol.* 12:5159–5173.
- Lee, M.S., R.C. Gallagher, J. Bradley, and E.H. Blackburn. 1993. In vivo and in vitro studies of telomeres and telomerase. *Cold Spring Harbor Symp. Quant. Biol.* 58:707–718.
- Lundblad, V., and E.H. Blackburn. 1993. An alternative pathway for yeast telomere maintenance rescues est1-senescence. *Cell*. 73:347–360.
- Lundblad, V., and J.W. Szostak. 1989. A mutant with a defect in telomere elongation leads to senescence in yeast. *Cell*. 57:633–643.
- McClintock, B. 1941. The stability of broken ends of chromosomes in *Zea Mays*. *Genetics*. 26:234–282.
- McEachern, M.J., and E.H. Blackburn. 1994. A conserved sequence motif within the exceptionally diverse telomeric sequences of budding yeasts. *Proc. Natl. Acad. Sci. USA*. 91:3453–3457.
- McEachern, M.J., and E.H. Blackburn. 1995. Runaway telomere elongation caused by telomerase RNA gene mutations. *Nature*. 376:403–409.
- McEachern, M.J., and E.H. Blackburn. 1996. Cap-prevented recombination between terminal telomeric repeat arrays (telomere CPR) maintains telomeres in *Kluyveromyces lactis* lacking telomerase. *Genes Dev.* 10:1822–1834.
- McEachern, M.J., and J.B. Hicks. 1993. Unusually large telomeric repeats in the yeast *Candida albicans*. *Mol. Cell. Biol.* 13:551–560.
- Moretti, P., K. Freeman, L. Coodly, and D. Shore. 1994. Evidence that a complex of SIR proteins interacts with the silencer and telomere-binding protein RAP1. *Genes Dev.* 8:2257–2269.
- Nimmo, E.R., A.L. Pidoux, P.E. Perry, and R.C. Allshire. 1998. Defective meiosis in telomere-silencing mutants of *Schizosaccharomyces pombe*. *Nature*. 392:825–828.
- Nugent, C.I., T.R. Hughes, N.F. Lue, and V. Lundblad. 1996. Cdc13p: a single-strand telomeric DNA-binding protein with a dual role in yeast telomere maintenance. *Science*. 274:249–252.
- Olovnikov, A.M. 1973. A theory of marginotomy. *J. Theor. Biol.* 41:181–190.
- Prescott, J., and E.H. Blackburn. 1997. Telomerase RNA mutations in *Saccharomyces cerevisiae* alter telomerase action and reveal nonprocessivity in vivo and in vitro. *Genes Dev.* 11:528–540.
- Romero, D.P., and E.H. Blackburn. 1995. Circular rDNA replicons persist in *Tetrahymena thermophila* transformants synthesizing GGGGTC telomeric repeats. *J. Eukaryot. Microbiol.* 42:32–43.
- Roy, J., T. Boswell-Fulton, and E.H. Blackburn. 1999. Specific telomerase RNA residues distant from the template are essential for telomerase function. *Genes Dev.* 12:3286–3300.
- Sandell, L.L., and V.A. Zakian. 1993. Loss of a yeast telomere: arrest, recovery, and chromosome loss. *Cell*. 75:729–739.
- Seoighe, C., and K.H. Wolfe. 1998. Extent of genomic rearrangement after genome duplication in yeast. *Proc. Natl. Acad. Sci. USA*. 95:4447–4452.
- Shampay, J., J.W. Szostak, and E.H. Blackburn. 1984. DNA sequences of telomeres maintained in yeast. *Nature*. 310:154–157.
- Singer, M.S., and D.E. Gottschling. 1994. TLC1: template RNA component of *Saccharomyces cerevisiae* telomerase. *Science*. 266:404–409.
- van Steensel, B., A. Smogorzewska, and T. de Lange. 1998. TRF2 protects human telomeres from end-to-end fusions. *Cell*. 92:401–413.
- Virta-Pearlman, V., D.K. Morris, and V. Lundblad. 1996. Est1 has the properties of a single-stranded telomere end-binding protein. *Genes Dev.* 10:3094–3104.
- Walmsley, R.M., and T.D. Petes. 1985. Genetic control of chromosome length in yeast. *Proc. Natl. Acad. Sci. USA*. 82:506–510.
- Walmsley, R.W., C.S. Chan, B.K. Tye, and T.D. Petes. 1984. Unusual DNA sequences associated with the ends of yeast chromosomes. *Nature*. 310:157–160.
- Watson, J.D. 1972. Origin of concatomeric T7 DNA. *Nat. New Biol.* 239:197–201.
- Wotton, D., and D. Shore. 1997. A novel Rap1p-interacting factor, Rif2p, cooperates with Rif1p to regulate telomere length in *Saccharomyces cerevisiae*. *Genes Dev.* 11:748–760.
- Yu, G.L., J.D. Bradley, L.D. Attardi, and E.H. Blackburn. 1990. In vivo alteration of telomere sequences and senescence caused by mutated *Tetrahymena* telomerase RNAs. *Nature*. 344:126–132.